Received: 13 September 2023 | Revised: 13 November 2023 | Accepted: 15 November 2023

DOI: 10.1002/dvg.23582

TECHNICAL REPORT

genesis WILEY

Generation of tamoxifen-inducible *Tfap2b-CreER^{T2}* mice using CRISPR-Cas9

Mingyi Zhang[1] | Jifan Feng[1] | Yue Li[2] | Peter Z. Qin[2] | Yang Chai[1]

[1]Center for Craniofacial Molecular Biology, University of Southern California, Los Angeles, California, USA

[2]Department of Chemistry, University of Southern California, Los Angeles, California, USA

Correspondence
Yang Chai, University Professor, George and MaryLou Boone Chair in Craniofacial Biology, Center for Craniofacial Molecular Biology, University of Southern California, 2250 Alcazar Street – CSA 103, Los Angeles, CA 90033, USA.
Email: ychai@usc.edu

Funding information
National Institute of Dental and Craniofacial Research; National Institutes of Health, Grant/Award Numbers: R01 DE022503, R01 DE012711; National Science Foundation, Grant/Award Number: MCB-1818107

Summary

Tfap2b, a pivotal transcription factor, plays critical roles within neural crest cells and their derived lineage. To unravel the intricate lineage dynamics and contribution of these Tfap2b+ cells during craniofacial development, we established a *Tfap2b-CreER^{T2}* knock-in transgenic mouse line using the CRISPR-Cas9-mediated homologous direct repair. By breeding with tdTomato reporter mice and initiating Cre activity through tamoxifen induction at distinct developmental time points, we show the *Tfap2b* lineage within the key neural crest-derived domains, such as the facial mesenchyme, midbrain, cerebellum, spinal cord, and limbs. Notably, the migratory neurons stemming from the dorsal root ganglia are visible subsequent to Cre activity initiated at E8.5. Intriguingly, Tfap2b+ cells, serving as the progenitors for limb development, show activity predominantly commencing at E10.5. Across the mouse craniofacial landscape, Tfap2b exhibits a widespread presence throughout the facial organs. Here we validate its role as a marker of progenitors in tooth development and have confirmed that this process initiates from E12.5. Our study not only validates the *Tfap2b-CreER^{T2}* transgenic line, but also provides a powerful tool for lineage tracing and genetic targeting of *Tfap2b*-expressing cells and their progenitor in a temporally and spatially regulated manner during the intricate process of development and organogenesis.

KEYWORDS
CRISPR-Cas9, mouse development, neural crest cell, *Tfap2b-CreER^{T2}*

1 | INTRODUCTION

The transcription factor AP-2β or TFAP2B serves as a vital transcription regulator expressed in the neural crest lineages during mouse embryogenesis. Expression of *Tfap2b* mRNA is detected in the neural tube, where neural crest cells originate, as early as E8.5 (Mitchell et al., 1991; Zhao et al., 2011). As development proceeds, the neural crest-derived dorsal root ganglia, epidermis, trigeminal ganglia, and facial mesenchyme as well as the pharyngeal arch, midbrain, and hindbrain all strongly express *Tfap2b* at E10.5 (Moser et al., 1997; Zhao et al., 2011). Moreover, additional investigations have established that Tfap2b is present in the limb bud and serves as a regulatory factor in limb development, in addition to its involvement in ductus arteriosus and aortic arch formation (Zhao et al., 2011). The expression of *Tfap2b* extends to other domains, including its role in mouse corneal endothelial cells during developmental stages, as well as its presence in the kidney, hair follicles, and olfactory epithelium (Hara et al., 2019; Moser et al., 1997). In adult tissues, the expression of *Tfap2b* is detectable in the spleen, kidney, and cerebellum. However, this expression is notably limited compared to the higher and more widespread levels observed during developmental stages (Mitchell et al., 1991). The information above indicates that Tfap2b is expressed

during various developmental stages and in adult tissues, where it performs its transcriptional regulatory functions.

In humans, *TFAP2B* mutation leads to the Char syndrome, an autosomal dominant disorder characterized by specific features such as patent ductus arteriosus, facial dysmorphism, abnormalities of the fifth finger, and dental anomalies (Char, 1978; Satoda et al., 2000; Tanasubsinn et al., 2017). Additionally, *TFAP2B* has been implicated in craniosynostosis (CS) and pathogenic mutations of *TFAP2B* could cause syndromic CS (Timberlake et al., 2019). Moreover, extensive studies have highlighted the significant roles of Tfap2b in the development, homeostasis, and tumorigenesis processes. It plays crucial roles in neural crest differentiation and specification, as well as in the differentiation of noradrenergic neurons in neuroblastoma, and in various aspects of cancer biology (Fu et al., 2014; Fu et al., 2019; Ikram et al., 2016; Rothstein & Simoes-Costa, 2020). Notably, TFAP2B+ cells give rise to the melanocyte stem cells in early development and tooth progenitor cells during tooth development (Brombin et al., 2022; Jing et al., 2022). Collectively, these studies underscore the indispensability of TFAP2B and emphasize the necessity of generating a CreERT2 line to specifically and temporally targeting Tfap2b+ cells.

The development of transgenic mouse lines with specific genetic modifications has been revolutionized by the CRISPR-Cas9 technology. The CRISPR-Cas9 system is utilized to precisely edit the mouse genome, introducing desired changes at targeted loci (Ran et al., 2013). To establish a transgenic mouse CreERT2 line through the utilization of the CRISPR-Cas9 technique, a single-guide RNA (sgRNA) is employed to guide the Cas9 enzyme to the precise genomic location of interest. The Cas9 enzyme then initiates a double-strand break at the designated site. This deliberate break prompts the cellular repair apparatus to engage, facilitating the incorporation of the desired DNA sequence via homologous direct repair (HDR) into the genome. This innovative approach has streamlined the process of creating genetically modified mice, allowing researchers to accurately and precisely dissect gene function and regulation.

In our study, we introduced the CreERT2 cassette within *Tfap2b* before the stop codon and validated the accuracy of this insertion under the control of the *Tfap2b* promoter. Moreover, we initiated the Cre activity at distinct embryonic development stages for the comparative analysis of *Tfap2b* expression and its lineage derivatives, and substantiated its expression in progenitor cells during tooth development. The tamoxifen-inducible *Tfap2b-CreER^{T2}* transgenic mouse presents an invaluable tool for dissecting Tfap2b+ cell trajectories during embryonic development and unraveling gene functions within this well-defined lineage.

2 | RESULTS

2.1 | Generation of tamoxifen-inducible *Tfap2b-CreER^{T2}* mice using CRISPR-Cas9

The mouse *Tfap2b* gene spans approximately 30 kb and is located on chromosome 1:19,279,132–19,309,071 (GRCm39: CM000994.3). Based on the cDNA sequencing results, it was revealed that Tfap2b comprises five distinct transcripts, three of which encode proteins. Notably, all three protein-coding transcripts exhibit a similar structural pattern comprising 7 or 8 exons (Ensembl, ENSMUSG00000025927; Kawai et al., 2001). Our strategy for generating a tamoxifen-inducible knock-in *Tfap2b-CreER^{T2}* line involved targeting exon 7 for insertion of the 2A-CreERT2 coding sequence near the stop codon (Figure 1a). Due to the existence of three *Tfap2b* transcripts with different exon 7 sequences and distinct stop codons, we designed a sgRNA to target a common sequence shared by all three transcripts, located proximal to the stop codon. A vector was meticulously prepared to facilitate the precise insertion, containing 500 bp left homology arm (LHA) and right homology arm (RHA) flanking the 2A-CreERT2 sequence. These homology arms, originating from the genomic site targeted by the gRNA, facilitate the precise homologous recombination of the desired sequence. Employing the powerful CRISPR-Cas9 technique, the sgRNA, vector, and Cas9 enzyme were introduced into the single-cell embryos through electroporation. The CRISPR-Cas9 system initiated a double-strand DNA break guided by the sgRNA, while the homology arms facilitated the insertion of the 2A-CreERT2 sequence at the intended target site through HDR. This process led to the induction of 2A-CreERT2 expression driven by the *Tfap2b* promoter, aligning with endogenous *Tfap2b* expression.

In order to identify transgenic mice with successful CreERT2 integration at the *Tfap2b* target site, we devised specific polymerase chain reaction (PCR) primers. These primers were designed to amplify a DNA fragment encompassing the CreERT2 cassette present within the donor construct, as well as a section of the *Tfap2b* gene located beyond the RHA (Figure 1b,c). The pair of primers we used was to confirm and validate that the CreERT2 sequence was specifically inserted into the target site. Out of a total of 22 pups examined, we successfully detected three transgenic *Tfap2b-CreER^{T2}* mice, each exhibiting the precise band size corresponding to the expected PCR product. This confirmed the accurate insertion of CreERT2 at the designated target site. We bred one of the founder mice with Bl6 females for three generations and used this as the founder line. Moreover, we also designed a set of tri-primer PCR reaction that can be used to identify the wide type, heterozygous, and homozygous CreERT2 insertion simultaneously (Figure 1d,e).

2.2 | Expression pattern of Tfap2b at different development time points

To investigate whether the Cre activity in the *Tfap2b-CreER^{T2}* mice could recapitulate the endogenous expression of *Tfap2b*, we generated *Tfap2b-CreER^{T2};tdTomato* reporter mice, with Cre activity induced at various developmental stages. The temporal dynamics of Cre activity were coordinated with the activation and synthesis of the tdTomato protein, which requires 24–48 h for full expression. As such, the mice in this study were examined within the initial 24–48 h following tamoxifen induction. To validate the fidelity of CreERT2 in representing endogenous *Tfap2b* expression, we first initiated Cre

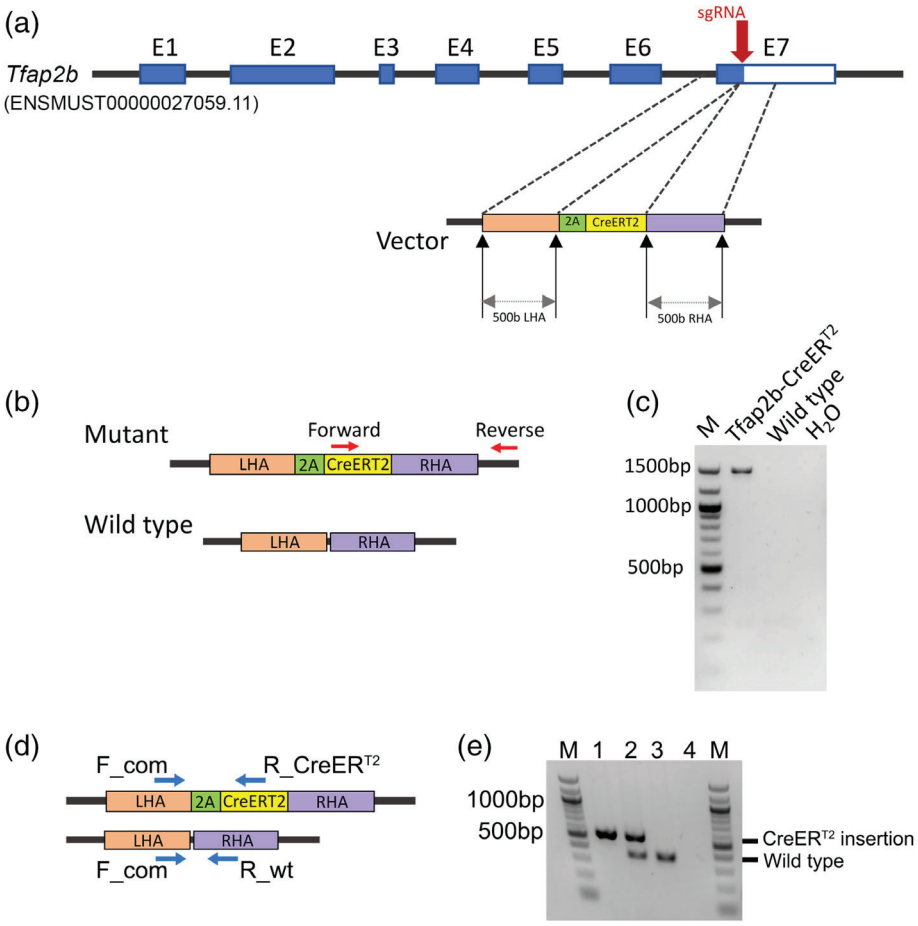

FIGURE 1 Strategy for generating *Tfap2b-CreER*^{T2} knock-in transgenic mice. (a) Schematic drawing of the knock-in strategy showing the insertion site within the *Tfap2b* gene and its donor composition. (b) Primer design and PCR product for the *Tfap2b-CreER*^{T2} transgenic line identification. Red arrows indicate the forward and reverse primer directions and positions within the genome. (c) PCR product for identifying the *Tfap2b-CreER*^{T2} transgenic. (d) Primer design for verifying the genotype among wild type, heterozygous, and homozygous *Tfap2b-CreER*^{T2} line. (e) PCR product for the primers verification. M, marker; 1, homozygous *Tfap2b-CreER*^{T2}; 2, heterozygous *Tfap2b-CreER*^{T2}; 3, wide type; 4, H2O. LHA, left homology arm; RHA, right homology arm. PCR, polymerase chain reaction.

activity via tamoxifen injection at E8.5, an embryonic time point previously identified as the onset of *Tfap2b* expression (Moser et al., 1997; Zhao et al., 2011). Subsequently, we collected embryos at E10.5 and conducted whole-embryo imaging. tdTomato expression was detected in the dorsal root ganglia, facial mesenchyme, and pharyngeal arches (Figure 2a–d). This result was consistent with previously published endogenous RNA detection of *Tfap2b* (Zhao et al., 2011), confirming the precision of the *Tfap2b-CreER*^{T2} line and its accurate reflection of the endogenous *Tfap2b* expression patterns in early neural crest cells.

Considering the dynamic and distinct endogenous expression profiles of *Tfap2b* across various embryonic development stages, we initiated Cre activity during later stages of development to comprehensively analyze its expression patterns. Specifically, tamoxifen induction was carried out at E10.5 and E12.5, followed by sample collections within 24–48 h. After tamoxifen induction at E10.5, samples collected at E12.5 revealed *Tfap2b* expression within pivotal embryonic structures, including the facial mesenchyme, trigeminal ganglia, hindbrain, midbrain, forelimbs, dorsal root ganglia, and spinal cord (Figure 2e–h). The sagittal section showed the tdTomato expression pattern in trigeminal ganglia, facial mesenchyme, spinal cord, and midbrain (Figure 2m). Tamoxifen induction at E12.5 and sample collection at E13.5 produced comparable tdTomato expression patterns to those initiated at E10.5, albeit with slightly reduced numbers of positive cells (Figure 2i–l). The in situ hybridization of *Tfap2b* at E12.5 represents the endogenous expression in the craniofacial part and shows that *Tfap2b* is expressed in the trigeminal ganglia, spinal cord, facial mesenchyme, and cerebellum (Figure 2n). The in situ hybridization of *Tfap2b* result showed a similar expression pattern with the lineage tracing results. Notably, these results underscore the ability of this transgenic line to label dorsal root ganglion cells by inducing Cre activity initiation prior to E8.5 or E10.5. Conversely, the cerebellum displayed heightened tdTomato-positive signals when Cre activity was initiated at E12.5 relative to initiation at E10.5 or earlier.

Collectively, our findings revealed the predominant expression of *Tfap2b* within neural crest-derived cells, notably in structures such as the facial mesenchyme, midbrain, cerebellum, and spinal cord, with minor variations based on the specific time point of Cre activity induction.

2.3 | Comparison of *Tfap2b* derivatives at E16.5 with different induction time points

To analyze the cellular derivatives of Tfap2b+ cells, we conducted a comparative analysis of tdTomato expression at E16.5 following Cre activity initiation at E8.5, E10.5, and E12.5. Upon examining E16.5 embryos induced at E8.5, we observed the most extensive tdTomato positive signals, spanning the entire craniofacial region including the

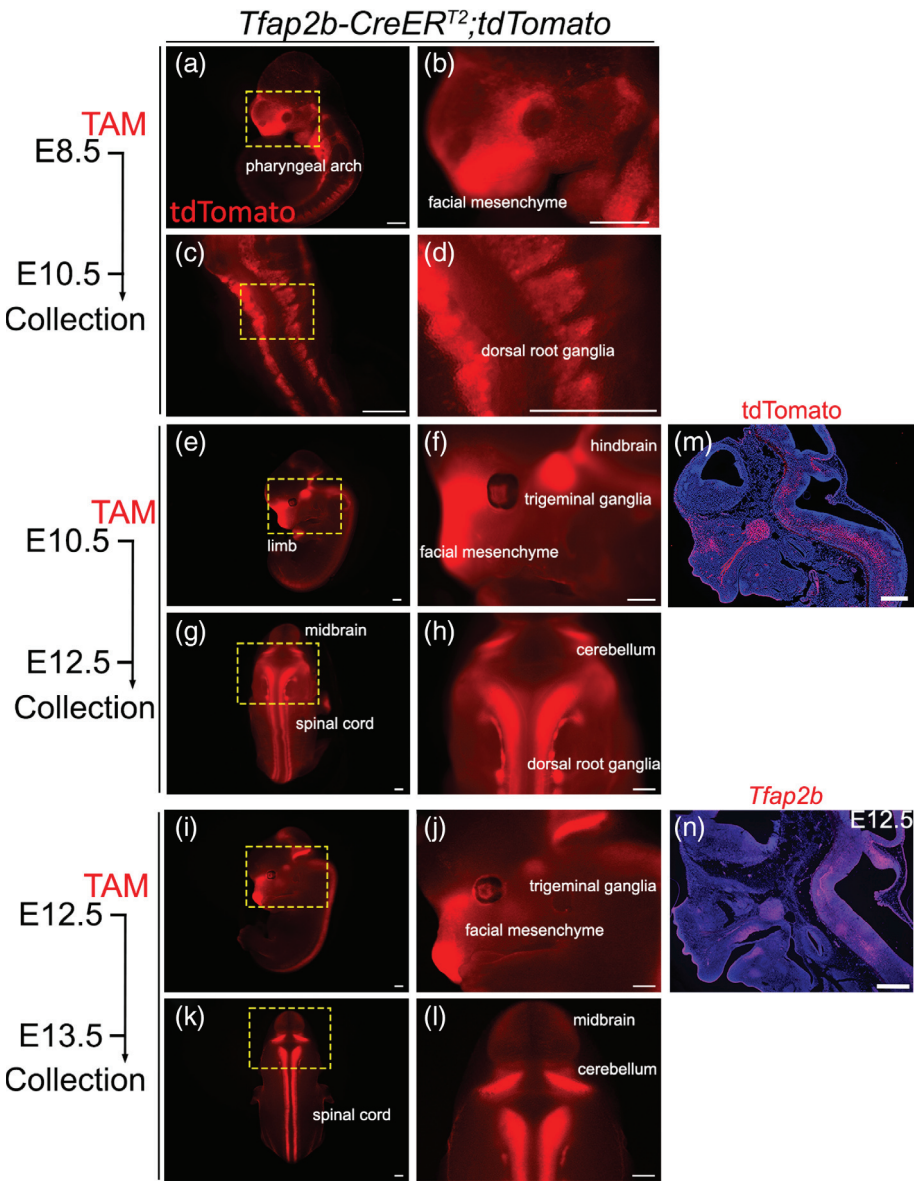

FIGURE 2 tdTomato expression patterns after initiating Cre activity at different time points. (a–d) Visualization of whole-mount *Tfap2b-CreER^{T2};tdTomato* mice 48 h post-tamoxifen induction at E8.5. (b) and (d) are high-magnification images of the boxes in (a) and (c), respectively. (e–h) Visualization of whole-mount *Tfap2b-CreER^{T2};tdTomato* mice 48 h post-tamoxifen induction at E10.5. (f) and (h) are high-magnification images of the boxes in (e) and (g) respectively. (i–l) Visualization of whole-mount *Tfap2b-CreER^{T2};tdTomato* mice 24 h post-tamoxifen induction at E12.5. (j) and (l) are high-magnification images of the boxes in (i) and (k), respectively. (m) Visualization of tdTomato expression of the sagittal section of E12.5 *Tfap2b-CreER^{T2};tdTomato* embryo after tamoxifen induction at E10.5. (n) *In situ* hybridization of *Tfap2b* at E12.5 embryo sample. The schematic indicates tamoxifen induction and harvest time points. Scale bar, 500 μm.

ears, eyes, and nasal structures. Intriguingly, signals were also identified in the hair follicles, limbs, cerebellum, midbrain, and spinal cord, as well as the neurons originating from the dorsal root ganglia (Figure 3a,d,g).

Tfap2b derivatives were detected within the facial mesenchyme, midbrain, cerebellum, spinal cord, and hair follicles at E16.5 after induction at each of the tested time points (Figure 3a–i). However, distinct variations in the distribution were discernible alongside the similarities. Notably, compared to lineage tracing initiated at E8.5, no tdTomato-positive signals were detected within migratory neurons when induction occurred at E10.5 and E12.5 (Figure 3d–f). Additionally, the presence of Tfap2b derivatives gradually diminished in the facial mesenchyme and ears following induction at time points from E8.5 to E12.5. Previous studies have reported that mouse forelimb development begins around E9.5, while hindlimb development initiates at around E10 (Martin, 1990; Wanek et al., 1989; Wang et al., 2022). Interestingly, when Cre activity was initiated at E8.5, only the forelimb tips exhibited a population of Tfap2b-derived cells. In contrast, tdTomato+ signals were detected in both forelimbs and hindlimbs when Cre activity was induced at E10.5 and E12.5 (Figure 3a–c). This data provides valuable insights into the dynamic expression of Tfap2b during limb development. This strategic approach facilitated a comprehensive understanding of the intricate spatiotemporal distribution of *Tfap2b* expressing cells and their derivatives across various stages of embryonic development.

2.4 | *Tfap2b-CreER^{T2}* efficiently targets the craniofacial organs when induced at E8.5

Our lineage tracing investigation revealed that Tfap2b+ derivatives effectively populate craniofacial organs at E14.5. To gain a comprehensive understanding of the distribution of the Tfap2b-derived populations within the craniofacial complex, we performed sectioning

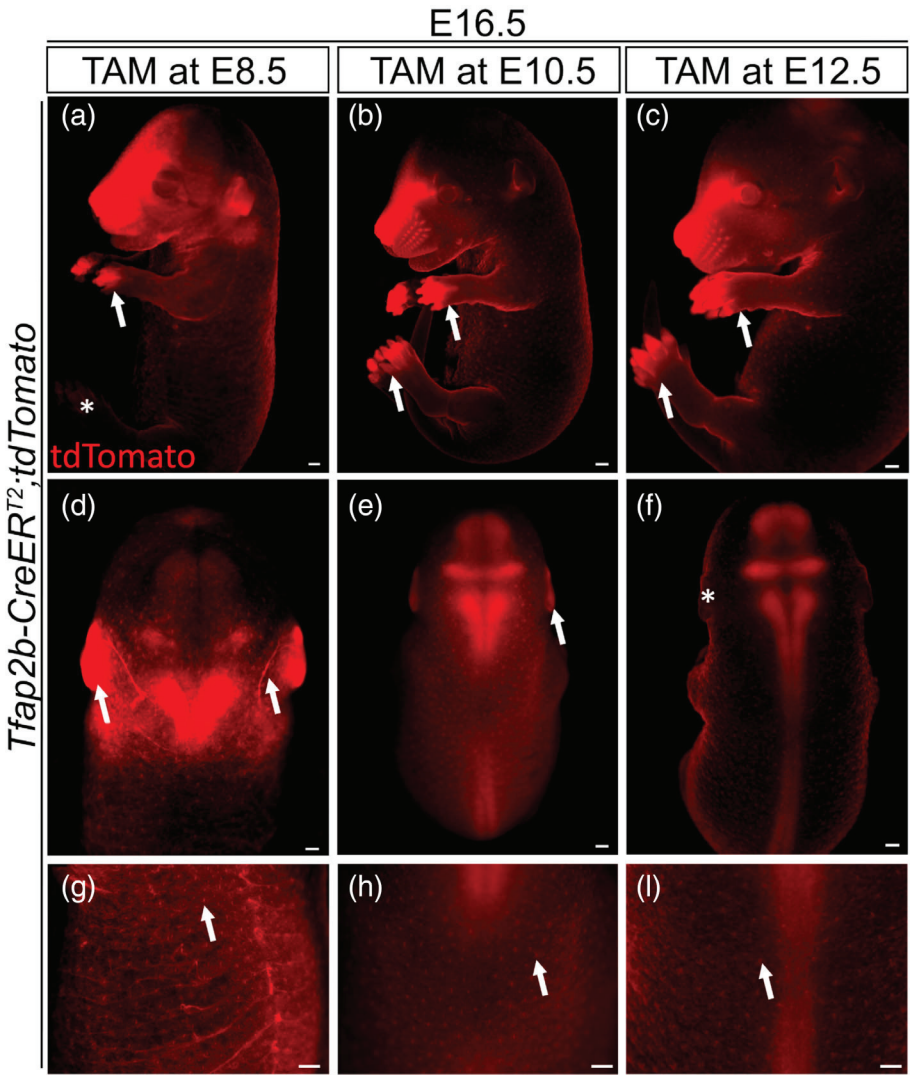

FIGURE 3 Comparison of tdTomato expression patterns at E16.5 after tamoxifen induction at distinct time points. (a and d) Visualization of whole-mount *Tfap2b-CreER^{T2};tdTomato* mice at E16.5 after tamoxifen induction at E8.5. (b and e) Visualization of whole-mount *Tfap2b-CreER^{T2};tdTomato* mice at E16.5 after tamoxifen induction at E10.5. (c and f) Visualization of whole-mount *Tfap2b-CreER^{T2};tdTomato* mice at E16.5 after tamoxifen induction at E12.5. (g–i) Visualization of the hair follicles for *Tfap2b-CreER^{T2};tdTomato* mice at E16.5 after tamoxifen induction at E8.5 (g), E10.5 (h), and E12.5 (i). Asterisks in (a, f) indicates the absence of the positive signals. Scale bar, 500 μm.

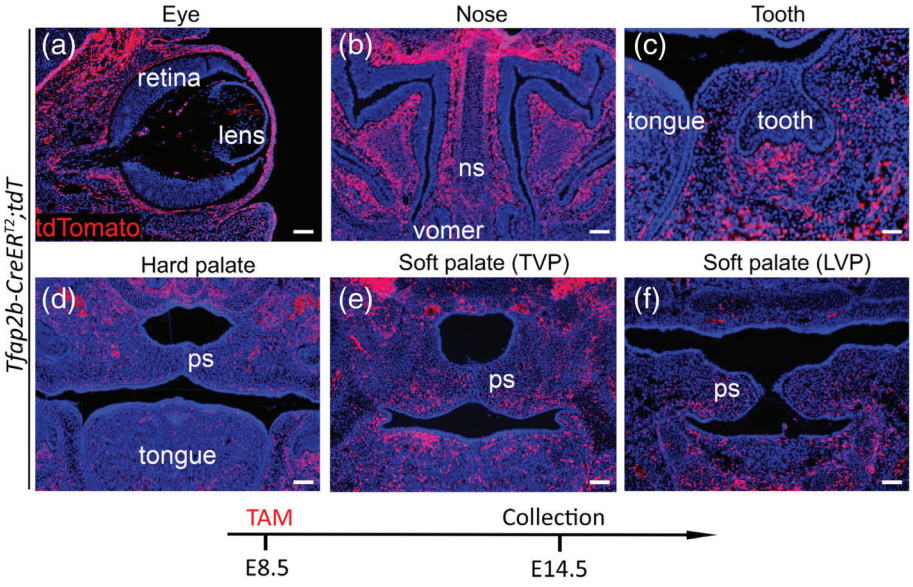

FIGURE 4 tdTomato expression in the craniofacial region of *Tfap2b-CreER^{T2};tdTomato* mice induced at E8.5. (a) Visualization of a coronal section of a *Tfap2b-CreER^{T2};tdTomato* mouse eye at E14.5. (b) Visualization of the nasal region of a *Tfap2b-CreER^{T2};tdTomato* mouse at E14.5. (c) Visualization of a *Tfap2b-CreER^{T2};tdTomato* mouse mandibular molar at E14.5. (d) Visualization of the hard palate region of a *Tfap2b-CreER^{T2};tdTomato* mouse at E14.5. (e and f) Visualization of the soft palatal shelf of a *Tfap2b-CreER^{T2};tdTomato* mouse at E14.5. ns, nasal septum; ps, palatal shelf; LVP, levator veli palatini; TVP, tensor veli palatini. The schematic indicates tamoxifen induction and harvest time points. Scale bar, 100 μm.

and visualization of the tdTomato expression within E14.5 embryos. Our observations showed that tdTomato+ cells were present within the facial mesenchyme-derived organs, such as the eyes, nose, and teeth, as well as the hard and soft palatal shelves (Figure 4a–f). These observations underscored the involvement of Tfap2b+ cells in the intricate process of craniofacial development.

2.5 | *Tfap2b-CreER^{T2}* efficiently labels cranial neural crest (CNC)-derived progenitors in the mouse molar when induced at E12.5

Research has identified the role of TFAP2B in human tooth development. Mutations in *TFAP2B* have been linked to various dental anomalies, including tooth agenesis, microdontia, supernumerary teeth, and root malformation (Tanasubsinn et al., 2017). In our previous study, *Tfap2b* was identified as a marker for early dental mesenchyme (Jing et al., 2022). These collective findings suggest a potential role of Tfap2b+ cells as a progenitor population contributing to tooth development. Anatomically, there are two distinct components of each molar tooth: the crown, which begins development during embryonic stages in the mouse, and the root, which begins development postnatally (Li et al., 2017). Embryonic molar development progresses sequentially through the bud (E13.5), cap (E14.5), and bell (E16.5) stages, while the postnatal phase involves tooth root development during which dental papilla and follicle lineages give rise to different parts of the tooth (Jing et al., 2022; Jussila & Thesleff, 2012; Yu & Klein, 2020). Specifically, dental papilla cells give rise to dental pulp and odontoblasts, whereas dental follicle cells differentiate into periodontal tissues including the periodontal ligament (PDL), cementum, and alveolar bone (Krivanek et al., 2017; Li et al., 2017). At P21.5, the process of tooth molar development is complete.

To test the hypothesis that Tfap2b+ cells are a population of CNC-derived progenitors during molar development, we performed lineage tracing with *Tfap2b-CreER^{T2};tdTomato* mice. Tamoxifen was administered at E12.5 to activate Cre activity, and samples were collected at different timepoints during tooth development. In Figure 5, tdTomato expression represents Tfap2b-positive cells and their derivatives after the induction of Cre activity. Tfap2b expression is observed in the dental mesenchyme at E13.5 (Figure 5a). Previously published scRNA-sequencing data revealed that the dental mesenchyme evolves into four distinct cellular domains at the bell stage (E16.5): the lateral follicle, apical follicle, coronal papilla, and apical papilla (Jing et al., 2022). Our lineage tracing confirmed that the tdTomato+ cells populated the entirety of the dental papilla and follicle domains (Figure 5b). By P0, tooth crown development is finalized, and the tooth is poised to undergo the crown-root transition which precedes root development. Consistent with the E16.5 lineage tracing result, both the dental papilla and follicle cells were confirmed to be Tfap2b-derived (Figure 5c). Subsequently, during tooth root development, the root furcation appeared concurrently with the elongation of the tooth roots, as well as the development of the PDL and alveolar bone. Notably, tdTomato-positive signals are evident in dental pulps, dental follicle, odontoblasts, alveolar bone, and PDL (Figure 5d–f). These findings indicate that Tfap2b serves as a marker for dental mesenchymal progenitor cells, and its derivatives encompass dental pulps, dental follicle, odontoblasts, alveolar bone, and PDL. Moreover, to explore the extent of Tfap2b+ cell distribution within the mandible, we collected the entire mandible and, following clearance procedures, specifically visualized tdTomato+ cells exclusively within the molar

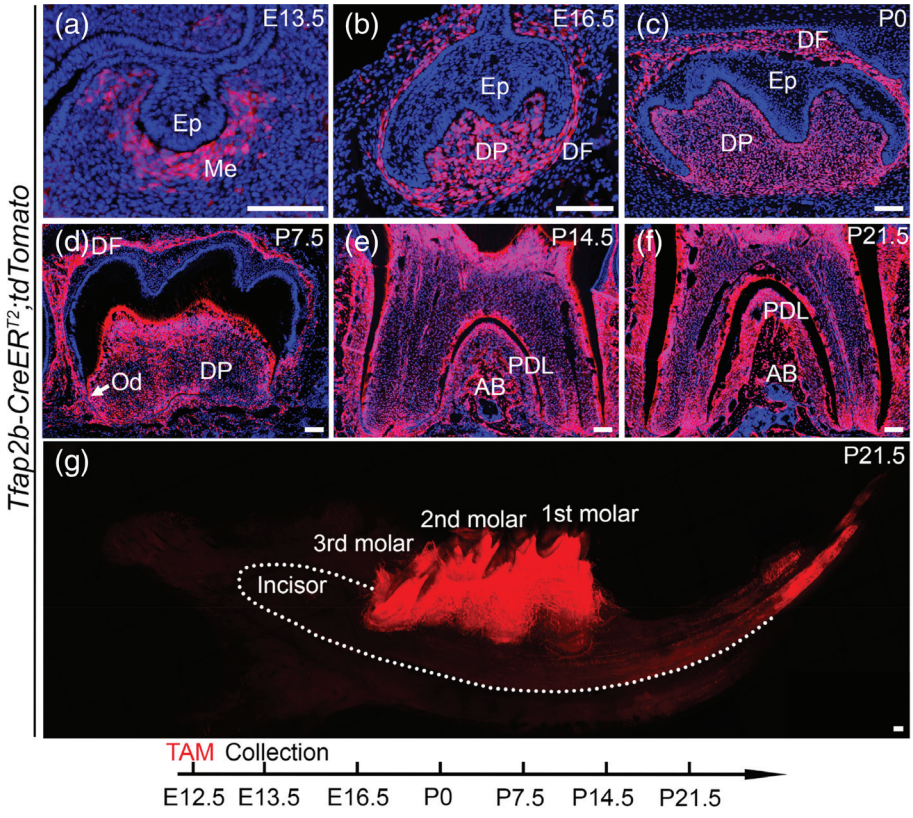

FIGURE 5 Tracing of the Tfap2b+ lineage during the tooth development of *Tfap2b-CreER^{T2};tdTomato* mice induced at E12.5. (a–f) Visualization of tdTomato expression during tooth development at E13.5 (a), E16.5 (b), P0 (c), P7.5 (d), P14.5 (e), and P21.5 (f). (g) Whole mandible visualization of tdTomato expression at P21.5 after tamoxifen induction at E12.5. The white dotted line outlines the mouse incisor. AB, alveolar bone; DF, dental follicle; DP, dental pulp; Ep, epithelia; Me, mesenchyme; Od, odontoblast; PDL, periodontal ligament. Scale bar, 100 μm.

region (Figure 5g). Collectively, these data strongly supported that Tfap2b+ cells serve as pivotal progenitor cells driving molar development.

3 | DISCUSSION

Our study describes the generation and validation of the *Tfap2b-CreER^{T2}* knock-in transgenic mouse model. By strategically inserting the CreERT2 sequence before the stop codon within *Tfap2b* gene, we established a reliable and inducible line for lineage tracing and genetic investigation of Tfap2b+ cells and their progeny. Tfap2b+ cells have been validated as progenitors for tooth development starting at E12.5. Taken together, our results demonstrate the precise spatiotemporal control afforded by this model, offering a powerful tool to delve deeper into the molecular mechanisms underlying Tfap2b-mediated developmental processes.

Generating transgenic mice is a powerful tool for molecular studies as it enables the validation of biological functions in vivo. Moreover, the specific CreERT2 lines allow for the dynamic investigation of its endogenous expression patterns and its specific lineages and derivatives, which are challenging to achieve through in vitro studies. With the advancements in CRISPR-Cas9 techniques, which have become the predominant approach for generating transgenic lines and conducting various studies, there are also concerns regarding off-target effects arise when employing genome editing techniques. In this regard, we designed a pair of primers, one from outside the homology arm and another targeting the CreERT2 region, to ensure the precise insertion of the target sequence into our intended site. Furthermore, it is noteworthy that the *Tfap2b-CreER^{T2}* knock-in transgenic mouse model exhibited normal viability and fertility.

The neural crest is formed during gastrulation, and after the neural fold formation, the transcription factor TFAP2 regulates neural crest specification (de Croze et al., 2011; Martik & Bronner, 2021). In the gastrula stage, the formation of TFAP2A and TFAP2C heterodimers triggers the activation of components within the neural plate border induction program. As neurulation ensues, TFAP2A/TFAP2B heterodimers promote neural crest specification by orchestrating a reconfiguration of the epigenetic landscape within the progenitor cells (Rothstein & Simoes-Costa, 2020). Subsequently, after the transition from neural crest specification to migratory neural crest cells, TFAP2B serves as a distinctive label for these cells. Furthermore, studies have established the involvement of Yap/Tead signaling in driving metabolic reprogramming, thus facilitating neural crest migration (Bhattacharya et al., 2020). Given that it has been established in the literature that *Tfap2b* RNA expression is detectable in mouse embryos as early as E8.5, we initiated our lineage tracing at this time point and were able to capture the migratory neurons at E14.5, enabling us to visualize this phenomenon in vivo.

Numerous studies have highlighted the essential roles of TFAP2B, not only in the various tissues affected by the Char syndrome, but also in the neural processes, tumorigenesis, and craniofacial development (Fu et al., 2014; Fu et al., 2019; Hu & Bringmann, 2023; Ikram et al., 2016; Satoda et al., 2000; Zhu et al., 2020). Our lineage tracing has revealed that Tfap2b+ cells are progenitors for tooth development. This investigation not only reaffirms the effectiveness of the generated *Tfap2b-CreER^{T2}* transgenic mouse model for lineage tracing but also yields valuable insights into the broader contributions of *Tfap2b*-expressing cell populations to diverse embryonic structures.

4 | METHODS

4.1 | Design of sgRNA and donor vector construct

To specifically target the 3′-end of *Tfap2b* near the stop codon, a sgRNA sequence (TATCTCACCGAGGCGCTCAA) was designed. pCAG-CreERT2 vector was obtained from Addgene (Plasmid #14797) for donor vector constriction (Feng et al., 2016; Matsuda & Cepko, 2007). The donor vector was engineered to incorporate a 5′ homology arm (500 bp), followed by the 2A sequence, CreERT2 sequence, and a 3′ homology arm (500 bp), which have been cloned into the vector (PNABio).

4.2 | Embryo electroporation injection

All animal procedures were performed according to NIH guidelines and approved by the University of Southern California Institutional Animal Care and Use Committee (IACUC). Embryo donors and foster mothers were sourced from B6D2F1 (C57BL/6 × DBA2) and CD-1 mouse strains, respectively. Super-ovulated female B6D2F1 mice, aged 8 weeks, were mated with B6D2F1 stud males and the fertilized embryos were collected from the oviducts.

Before the injection, 20 ng/μL Cas9 Nuclease v3 (IDT, 1081058) and *Tfap2b* sgRNA (0.61 pmol/μL crRNA + 0.61 pmol/μL trancrRNA) were combined on ice and put into a 37°C oven for 10 min. Following this, purified *Tfap2b* donor vector (5–10 ng/mL) was added into the mixture. Subsequently, the mixture was carefully injected into both the cytoplasm and the pronuclei of fertilized eggs exhibiting well-defined pronuclei. These injections were carried out in M2 medium (M2112, Cytospreen). The eggs were then incubated overnight at 37.8°C in 5% CO_2 in M16 medium (M6111, Cytospreen). Ultimately, around 20–25 two-cell stage embryos were successfully transplanted into the oviducts of pseudopregnant CD-1 females at 0.5 days post coitum (dpc).

4.3 | *Tfap2b-CreER^{T2}* founder mouse identification

Tfap2b-CreER^{T2} transgenic knock-in mice were identified by genotyping the PCR product which targets the CreERT2 to the downstream region of the 3′ homology arm to confirm that the target region was successfully inserted to the targeted position. The forward primer used was 5′-AACGTGGTGCCCCTCTATGA-3′ and the reverse primer was 5′-GATACCTTACTCGACTCCCTT-3′, with a 1521 bp PCR product. Three *Tfap2b-CreER^{T2}* mice were identified from 22 pups.

The tri-primer set was used to identify the genotype of the *Tfap2b-CreER^{T2}* line. The common forward primer was 5′-ACTTCAGTCTCATCACGCAC-3′, the wild type of reverse primer was 5′-TTTGTTGCTCCGTTGTATGCC-3′, and the CreERT2 reverse primer was 5′-GGCCCAAATGTTGCTGGATAG-3′, with the 385 bp wild type PCR product and 543 bp CreERT2 PCR product.

4.4 | Tamoxifen administration

To prepare the injection agent, tamoxifen (Sigma-Aldrich, T5648) and corn oil (Sigma-Aldrich, C8267) were mixed to achieve a concentration of 20 mg/mL. We checked plug for tdTomato female mice which paired with *Tfap2b-CreER^{T2}* male mouse, and the plugged female mice were intraperitoneally injected with tamoxifen at the specific date with a single dosage of 1.5 mg/10 g body weight.

4.5 | Lineage tracing and genetic labeling

*ROSA26*LoxP-STOP-LoxP-tdTomato (tdTomato) female reporter mice were crossed with the *Tfap2b-CreER^{T2}* mice. The tdTomato mice were obtained from the Jackson Laboratory (JAX no. 007905) (Madisen et al., 2010). The mated tdTomato females received tamoxifen injections at E8.5, E10.5, and E12.5, and then were euthanized at least 24 h post-induction to collect the *Tfap2b-CreER^{T2};tdTomato* embryos. Whole-body imaging was performed using a Leica MZ10F.

4.6 | Sample preparation and cryosection

The collected embryos were fixed in 10% formalin solution (Sigma, HT501128) at 4°C overnight and dehydrated in sucrose/PBS solutions of increasing concentrations (15%, 30%, and sucrose/OCT), before being embedded in OCT compound. The samples were sliced into 8 μm sections with a cryostat (Leica CM1850) and collected onto slides. Then the sliced samples were counterstained with DAPI (Thermo Fisher Scientific, 62248) and then mounted.

4.7 | In situ hybridization

In situ hybridization was performed using the RNAscope Multiples fluorescent v2 kit (Advanced Cell Diagnosis, 323100) according to the manufacturer's instructions. The probes used in this study were synthesized by Advanced Cell Diagnostics: Probe-Mm-*Tfap2b*-O1 (535151). All the images were captured with a fluorescence microscope (Keyence, BZ-X810).

4.8 | Mandible clearance process

The collected mandibles were fixed in 10% formalin solution (Sigma, HT501128) at 4°C overnight. The fixed mandibles underwent decalcification in 10% DEPC-EDTA for 2 weeks and rinsed in PBS three times, in preparation for the process of the clearance following the manufacturer's instructions (TCI, Tissue-clearing reagent CUBIC T3740 and T3741). The mandible samples were imaged using a Stellaris confocal microscope (Leica).

AUTHOR CONTRIBUTIONS

Mingyi Zhang and Yang Chai designed the study; Mingyi Zhang carried out most of the experiments and data analysis; Jifan Feng, Yue Li, and Peter Z. Qin participated in project design and sample collection. Mingyi Zhang and Yang Chai cowrote the paper. Yang Chai supervised the research.

ACKNOWLEDGMENTS

We acknowledge Dr. Bridget Samuels for critical reading and editing of the manuscript, and Nancy Wu from USC Norris Comprehensive Cancer Center Transgenic/Knockout Rodent Core Facility for technical supports of the electroporation process. This study was supported by grant funding from the National Institute of Dental and Craniofacial Research, National Institutes of Health (R01 DE012711 and R01 DE022503 to Y.C.), and National Science Foundation (MCB-1818107 to P.Z.Q.).

ORCID

Yang Chai https://orcid.org/0000-0003-2477-7247

REFERENCES

Bhattacharya, D., Azambuja, A. P., & Simoes-Costa, M. (2020). Metabolic reprogramming promotes neural crest migration via yap/Tead signaling. *Developmental Cell*, *53*, 199–211, e196.

Brombin, A., Simpson, D. J., Travnickova, J., Brunsdon, H., Zeng, Z., Lu, Y., Young, A. I. J., Chandra, T., & Patton, E. E. (2022). Tfap2b specifies an embryonic melanocyte stem cell that retains adult multifate potential. *Cell Reports*, *38*, 110234.

Char, F. (1978). Peculiar facies with short philtrum, duck-bill lips, ptosis and low-set ears—A new syndrome? *Birth Defects Original Article Series*, *14*, 303–305.

de Croze, N., Maczkowiak, F., & Monsoro-Burq, A. H. (2011). Reiterative AP2a activity controls sequential steps in the neural crest gene regulatory network. *Proceedings of the National Academy of Sciences of the United States of America*, *108*, 155–160.

Feng, J., Jing, J., Sanchez-Lara, P. A., Bootwalla, M. S., Buckley, J., Wu, N., Yan, Y., & Chai, Y. (2016). Generation and characterization of tamoxifen-inducible Pax9-CreER knock-in mice using CrispR/Cas9. *Genesis*, *54*, 490–496.

Fu, L., Shi, K., Wang, J., Chen, W., Shi, D., Tian, Y., Guo, W., Yu, W., Xiao, X., Kang, T., Wang, S., Huang, W., & Deng, W. (2014). TFAP2B overexpression contributes to tumor growth and a poor prognosis of human lung adenocarcinoma through modulation of ERK and VEGF/PEDF signaling. *Molecular Cancer*, *13*, 89.

Fu, X., Zhang, H., Chen, Z., Yang, Z., Shi, D., Liu, T., Chen, W., Yao, F., Su, X., Deng, W., Chen, M., & Yang, A. (2019). TFAP2B overexpression contributes to tumor growth and progression of thyroid cancer through the COX-2 signaling pathway. *Cell Death & Disease*, *10*, 397.

Hara, S., Kawasaki, S., Yoshihara, M., Winegarner, A., Busch, C., Tsujikawa, M., & Nishida, K. (2019). Transcription factor TFAP2B upregulates human corneal endothelial cell-specific genes during corneal development and maintenance. *The Journal of Biological Chemistry*, *294*, 2460–2469.

Hu, Y., & Bringmann, H. (2023). Tfap2b acts in GABAergic neurons to control sleep in mice. *Scientific Reports*, *13*, 8026.

Ikram, F., Ackermann, S., Kahlert, Y., Volland, R., Roels, F., Engesser, A., Hertwig, F., Kocak, H., Hero, B., Dreidax, D., Henrich, K. O., Berthold, F., Nürnberg, P., Westermann, F., & Fischer, M. (2016). Transcription factor activating protein 2 beta (TFAP2B) mediates noradrenergic neuronal differentiation in neuroblastoma. *Molecular Oncology*, *10*, 344–359.

Jing, J., Feng, J., Yuan, Y., Guo, T., Lei, J., Pei, F., Ho, T. V., & Chai, Y. (2022). Spatiotemporal single-cell regulatory atlas reveals neural crest lineage diversification and cellular function during tooth morphogenesis. *Nature Communications*, *13*, 4803.

Jussila, M., & Thesleff, I. (2012). Signaling networks regulating tooth organogenesis and regeneration, and the specification of dental mesenchymal and epithelial cell lineages. *Cold Spring Harbor Perspectives in Biology*, *4*, a008425.

Kawai, J., Shinagawa, A., Shibata, K., Yoshino, M., Itoh, M., Ishii, Y., Arakawa, T., Hara, A., Fukunishi, Y., Konno, H., Adachi, J., Fukuda, S., Aizawa, K., Izawa, M., Nishi, K., Kiyosawa, H., Kondo, S., Yamanaka, I., Saito, T., … RIKEN Genome Exploration Research Group Phase II Team and the FANTOM Consortium. (2001). Functional annotation of a full-length mouse cDNA collection. *Nature*, *409*, 685–690.

Krivanek, J., Adameyko, I., & Fried, K. (2017). Heterogeneity and developmental connections between cell types inhabiting teeth. *Frontiers in Physiology*, *8*, 376.

Li, J., Parada, C., & Chai, Y. (2017). Cellular and molecular mechanisms of tooth root development. *Development*, *144*, 374–384.

Madisen, L., Zwingman, T. A., Sunkin, S. M., Oh, S. W., Zariwala, H. A., Gu, H., Ng, L. L., Palmiter, R. D., Hawrylycz, M. J., Jones, A. R., Lein, E. S., & Zeng, H. (2010). A robust and high-throughput Cre reporting and characterization system for the whole mouse brain. *Nature Neuroscience*, *13*, 133–140.

Martik, M. L., & Bronner, M. E. (2021). Riding the crest to get a head: Neural crest evolution in vertebrates. *Nature Reviews. Neuroscience*, *22*, 616–626.

Martin, P. (1990). Tissue patterning in the developing mouse limb. *The International Journal of Developmental Biology*, *34*, 323–336.

Matsuda, T., & Cepko, C. L. (2007). Controlled expression of transgenes introduced by in vivo electroporation. *Proceedings of the National Academy of Sciences of the United States of America*, *104*, 1027–1032.

Mitchell, P. J., Timmons, P. M., Hebert, J. M., Rigby, P. W., & Tjian, R. (1991). Transcription factor AP-2 is expressed in neural crest cell lineages during mouse embryogenesis. *Genes & Development*, *5*, 105–119.

Moser, M., Ruschoff, J., & Buettner, R. (1997). Comparative analysis of AP-2 alpha and AP-2 beta gene expression during murine embryogenesis. *Developmental Dynamics*, *208*, 115–124.

Ran, F. A., Hsu, P. D., Wright, J., Agarwala, V., Scott, D. A., & Zhang, F. (2013). Genome engineering using the CRISPR-Cas9 system. *Nature Protocols*, *8*, 2281–2308.

Rothstein, M., & Simoes-Costa, M. (2020). Heterodimerization of TFAP2 pioneer factors drives epigenomic remodeling during neural crest specification. *Genome Research*, *30*, 35–48.

Satoda, M., Zhao, F., Diaz, G. A., Burn, J., Goodship, J., Davidson, H. R., Pierpont, M. E., & Gelb, B. D. (2000). Mutations in TFAP2B cause Char syndrome, a familial form of patent ductus arteriosus. *Nature Genetics*, *25*, 42–46.

Tanasubsinn, N., Sittiwangkul, R., Pongprot, Y., Kawasaki, K., Ohazama, A., Sastraruji, T., Kaewgahya, M., & Kantaputra, P. N. (2017). TFAP2B mutation and dental anomalies. *Journal of Human Genetics*, *62*, 769–775.

Timberlake, A. T., Jin, S. C., Nelson-Williams, C., Wu, R., Furey, C. G., Islam, B., Haider, S., Loring, E., Galm, A., Yale Center for Genome Analysis, Steinbacher, D. M., Larysz, D., Staffenberg, D. A., Flores, R. L., Rodriguez, E. D., Boggon, T. J., Persing, J. A., & Lifton, R. P. (2019). Mutations in TFAP2B and previously unimplicated genes of the BMP, Wnt, and hedgehog pathways in syndromic craniosynostosis. *Proceedings of the National Academy of Sciences of the United States of America*, *116*, 15116–15121.

Wanek, N., Muneoka, K., Holler-Dinsmore, G., Burton, R., & Bryant, S. V. (1989). A staging system for mouse limb development. *The Journal of Experimental Zoology*, *249*, 41–49.

Wang, M., Jiang, R., Tan, G., Liu, Z., Tang, C., Wu, R., & Shi, D. (2022). Identification of transcription factor networks during mouse hindlimb development. *Cell*, *12*, 28.

Yu, T., & Klein, O. D. (2020). Molecular and cellular mechanisms of tooth development, homeostasis and repair. *Development*, *147*, dev184754.

Zhao, F., Bosserhoff, A. K., Buettner, R., & Moser, M. (2011). A heart-hand syndrome gene: Tfap2b plays a critical role in the development and remodeling of mouse ductus arteriosus and limb patterning. *PLoS One*, *6*, e22908.

Zhu, M., Zou, L., Lu, F., Ye, L., Su, B., Yang, K., Lin, M., Fu, J., & Li, Y. (2020). miR-142-5p promotes renal cell tumorigenesis by targeting TFAP2B. *Oncology Letters*, *20*, 324.

How to cite this article: Zhang, M., Feng, J., Li, Y., Qin, P. Z., & Chai, Y. (2023). Generation of tamoxifen-inducible *Tfap2b-CreER*^{T2} mice using CRISPR-Cas9. *genesis*, e23582. https://doi.org/10.1002/dvg.23582